Experimental conversion of position correlation into polarization entanglement

Chithrabhanu Perumangatt and Alexander Lohrmann
Centre for Quantum Technologies, National University of Singapore, 3 Science Drive 2, Singapore S117543, Singapore

Alexander Ling
Centre for Quantum Technologies, National University of Singapore, 3 Science Drive 2, Singapore S117543, Singapore
and Department of Physics, National University of Singapore, 2 Science Drive 3, Singapore S117542, Singapore

(Received 26 October 2019; accepted 29 May 2020; published 6 July 2020)

This paper presents a method to convert position correlation of photon pairs into polarization entanglement. This is achieved by individually manipulating the polarization state of photons generated in different parts of a nonlinear medium and coherently superposing them. This concept is experimentally demonstrated using photon pairs produced by spontaneous parametric down-conversion. The method is used to implement a compact source producing an observed photon-pair rate of 120 000 s^{-1}/mW with an entanglement fidelity of 0.991 ± 0.013. This method can be extended to any photon-pair generation process with initial position correlation.

DOI: 10.1103/PhysRevA.102.012404

I. INTRODUCTION

Photons entangled in polarization have been a prime tool for experiments in fundamental quantum physics [1–5] and they are an essential part of many quantum communication schemes [6–8]. One of the most mature methods to create such photons is using spontaneous parametric down-conversion (SPDC), where a pump photon splits into two lower-energy photons under conservation of energy and momentum in a nonlinear crystal. To generate polarization entanglement from SPDC, it is necessary to impose coherent superposition of two pump-decay paths.

There is a variety of techniques by which this coherent superposition can be achieved. Examples of previous entangled photon-pair sources have utilized momentum correlation [9], indistinguishable pump decay in two separate crystals [10–13], or two distinguishable pump beams [14–19]. The correlation in the birth position of the photon pairs [20] is yet another property that can potentially be exploited for the generation of polarization entanglement. Position correlation is an intrinsic property of photon pairs produced in any parametric process in a bulk medium. This position correlation is independent of the phase matching used in SPDC and is preserved unless it is filtered into a single spatial mode. Position and momentum correlations can be exploited for higher-dimensional entanglement and are used for sensing and imaging applications [21–23].

This paper reports the use of position correlation to implement high-quality polarization entangled photon-pair sources. In this method, the polarization state of the photons produced at corresponding transverse positions in the nonlinear crystal is manipulated before undergoing coherent superposition. A proof-of-concept demonstration is first performed by implementing a modified Mach-Zehnder interferometer for the manipulation and superposition. Next the technique was applied to implement a bright entangled photon-pair source with minimum elements in a simple geometry. This technique can also be extended to other pair production processes such as four-wave mixing in an atomic vapor [24,25].

II. CONCEPT AND EXPERIMENTAL DEMONSTRATION

Consider collinear type-0 SPDC ($H \rightarrow HH$) in a periodically poled crystal where the pump, signal, and idler photons are copolarized. The birth position of a photon pair can be anywhere within the interaction volume. These positions are discretized into two bins by labels x_1 and x_2 [see the close-up of the SPDC interaction volume in Fig. 1(a)] according to their origin with respect to a conceptual line drawn through the center of the interaction volume. The states generated in each discrete space can be written as

$$|\phi_1\rangle = |x_1, x_1\rangle \otimes |HH\rangle, \quad |\phi_2\rangle = |x_2, x_2\rangle \otimes |HH\rangle, \tag{1}$$

where 1 and 2 correspond to the different transverse positions and $|HH\rangle$ indicates the horizontal polarization state of the photons. A polarization transformation $|HH\rangle \rightarrow |VV\rangle$ is applied to photons with the state $|\phi_2\rangle$ ($|\phi_2\rangle \rightarrow |\phi_2'\rangle$). The states $|\phi_1\rangle$ and $|\phi_2'\rangle$ are coherently superposed via a polarizing beam splitter (PBS). The resultant state can be written as

$$|\phi\rangle = \frac{1}{\sqrt{2}}(|x_1, x_1\rangle \otimes |HH\rangle + e^{i\Delta\varphi}|x_2 x_2\rangle \otimes |VV\rangle). \tag{2}$$

The photons are then projected into a single mode erasing any position distinguishability. The state after the single-mode projection is given by

$$|\phi\rangle = \frac{1}{\sqrt{2}}(|HH\rangle + e^{i\Delta\varphi}|VV\rangle). \tag{3}$$

By adjusting the constant phase offset $\Delta\varphi$, the maximally entangled Bell states $|\Phi^{\pm}\rangle$ can be generated.

An implementation of the concept using a Mach-Zehnder interferometer is shown in Fig. 1(a). A laser beam of 405 nm with a 160-MHz linewidth is focused (pump waist of 150 μm) into a periodically poled potassium titanyl phosphate

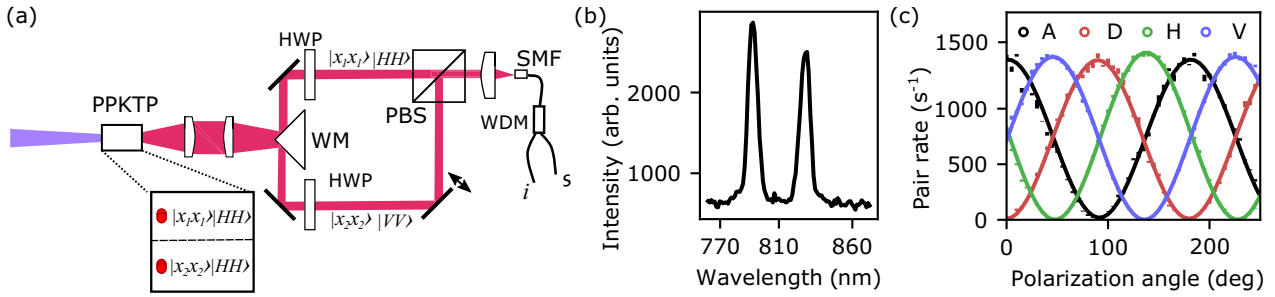

FIG. 1. (a) Experimental setup for the conversion of position correlation to polarization entanglement. The close-up of the SPDC interaction volume describes photon pairs generated at the upper part of the crystal having position state $|x_1, x_1\rangle$, while photon pairs generated on the lower part are marked as $|x_2, x_2\rangle$. Two planoconvex lenses ($f = 15$ mm) are used to image the interaction volume onto a wedge mirror (WM). The photons are coupled into a single-mode fiber (SMF) and a wavelength division multiplexer is used to split the signal (s) and idler (i) photons. A mirror inside the interferometer is attached to a piezoactuator to lock the phase while observing the constructive or destructive interference fringe produced by the pump laser. (b) Measured spectrum of the SPDC photons. (c) Two-photon polarization correlation curves of the photon pairs demonstrating high visibility. The signal photon is projected to four linear polarization states. A, D, H, and V correspond to different polarizer settings (polarizer oriented at 45°, 135°, 0°, and 90°) that project the single-photon polarization state into antidiagonal, diagonal, horizontal, and vertical polarizations. Error bars correspond to the standard deviation of the detected photon count rate.

(PPKTP) crystal with a length of 10 mm, kept in an oven to regulate the temperature. Nondegenerate, collinear type-0 phase matching is employed for the generation of photon pairs. The nondegenerate condition is used since the final separation of the signal and idler photons is done by wavelength. The crystal temperature is tuned to generate signal and idler wavelengths at 792 and 829 nm, respectively, as shown in Fig. 1(b). For exploiting the position correlation, the center of the crystal (SPDC interaction volume) is imaged onto a wedge mirror using two planoconvex lenses in a $4f$ configuration [21,23]. The effective collection waist at the center of the crystal is 75 μm. The wedge mirror splits the SPDC photons according to the birth position.

The polarization state of the photons reflected to the downward path is converted from horizontal to vertical using a half waveplate (HWP). The polarization of the photons reflected to the upward path is not rotated. Nevertheless, they pass through a HWP oriented at 0° for matching the dispersion experienced by photons in the upper path. Both beams are combined using a polarizing beam splitter and then coupled to a single-mode fiber. The signal and idler photons are then separated using a wavelength division multiplexer (WDM). The phase difference between horizontally and vertically polarized photon pairs, before reaching the PBS, is $\Delta\varphi = 2\pi\,\Delta L(\frac{1}{\lambda_s} + \frac{1}{\lambda_i}) = 2\pi\,\Delta L(\frac{1}{\lambda_p})$, where λ_p and ΔL are the pump wavelength and path length difference, respectively. To get a 0 or π phase, the interferometer is locked onto either the constructive or destructive interference fringe produced by the pump beam.

The photons exiting the WDM are detected on Geiger mode avalanche photodiodes (SAP500) with efficiencies of approximately 40%–50%. The observed pair rate normalized to pump power is 260 k/s/mW with pair-to-singles ratios of 20% and 16% for signal and idler photons, respectively. The polarization state of the signal and idler photons are analyzed for their nonlocal polarization correlations. The photon-pair polarization correlation curves are given in Fig. 1(c) and exhibit an average visibility of 0.995 ± 0.013 with a corresponding [26] fidelity of 0.997 ± 0.013 towards the maximally entangled $|\Phi^+\rangle$ state.

The quality of the state depends upon the imaging system. In a nonideal imaging system, for example, when the wedge mirror is displaced from the focal position of the second lens, some of the SPDC photons will be separated by momentum rather than position. This can introduce polarization anticorrelation resulting in a reduction in entanglement fidelity. Shifts in the transverse position of the wedge mirror can also result in a nonmaximally entangled state.

This interferometer setup could be used to generate anticorrelated $|\Psi^\pm\rangle$ Bell states. This can be done by utilizing momentum correlation and is achieved when a $2f$ lens system is used. This method splits the photon pair; instead of two photons going into either arm, the twin photons are separated at the wedge mirror and traverse each arm singly. With this setup, however, it is difficult to achieve high fidelity because the phase difference is now proportional to $\Delta L(\frac{1}{\lambda_s} - \frac{1}{\lambda_i})$. Since the signal and idler wavelengths intrinsically have a broad bandwidth as shown in Fig. 1(b) (unless strong wavelength filtering is used, which in turn has a strong impact on brightness), generation of high-quality $|\Psi^\pm\rangle$ states requires the absolute path length difference in the current implementation to be less than tens of microns.

III. COMPACT SOURCE

The inherent instability of the Mach-Zehnder-type interferometer makes it challenging to deploy the source in a rugged environment [27]. Alternatively, one can implement the method using a folded Mach-Zehnder interferometer, which offers better stability since photons in both paths are reflected by the same mirror. A compact design that is intrinsically more stable is shown in Fig. 2(a). In this approach the PPKTP crystal is pumped with a collimated beam and the generated SPDC photon pairs undergo polarization treatment as soon as they exit the crystal. The photon pairs, after undergoing polarization manipulation, are coherently superposed using the walkoff in a nonlinear crystal and coupled into a single-mode fiber.

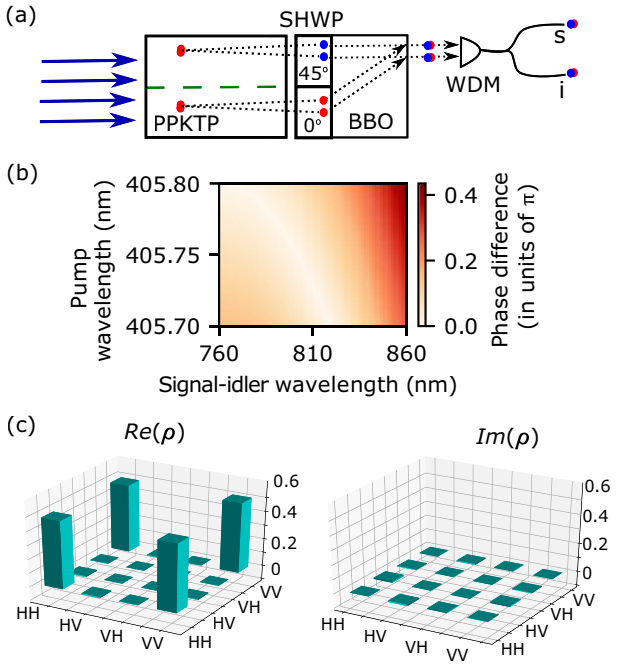

FIG. 2. (a) Schematic of the compact polarization entangled photon source. The dashed lines represent the distinction between photons generated at different parts of the PPKTP crystal. Red and blue closed circles represent horizontally and vertically polarized photons, respectively. The WDM separates the photon pairs according to its wavelength. (b) Phase difference between $|HH\rangle$ and $|VV\rangle$ states for different pump and signal wavelengths. (c) Real and imaginary parts of the density matrix for the state generated using the compact setup.

In the actual implementation, a collimated pump beam with a waist size of approximately 400 μm is used. The SPDC photons pass through an achromatic segmented half waveplate (SHWP) placed at the exit face of the PPKTP crystal. One half of the SHWP is oriented at 45°, while the other half is oriented at 0°. The use of a segmented half waveplate is convenient since the total phase acquired in both paths will be approximately equal.

To combine the two paths, the source uses a β barium borate (BBO) crystal with a cut angle of 28.8° and a length of 4 mm. The length of the nonlinear crystal is chosen such that it introduces a displacement that is half the pump beamwidth. The superposed photons are then collected into a single-mode fiber before being separated according to their wavelength. The effective collection waist at the center of the crystal is 75 μm.

Spatial walkoff for the coherent superposition of SPDC from two separate copropagating pump beams has been used in previous work for the generation of polarization entanglement [17–19]. A major difference of this work from previous reports is that the source under discussion requires only a single pump beam and the two decay paths are generated conceptually from a single SPDC interaction volume.

Compared to the free-space interferometer, there is a wavelength-dependent phase [Fig. 2(b)] introduced by the BBO crystal which has a chromatic birefringence. In principle, it could be corrected using a positive uniaxial crystal, e.g. yttrium orthovanadate. However, the SPDC spectrum is sufficiently narrow [see Fig. 1(b)] and the corresponding phase is negligible. The constant phase $\Delta\varphi$, due to the relative path length difference between $|HH\rangle$ and $|VV\rangle$ states, is corrected by tilting the BBO crystal. One could also tune this constant phase actively by introducing a liquid crystal retarder [28].

With the compact source, the observed brightness is 120 k/s/mW with pair-to-singles ratios of 18% and 15% for the signal and idler, respectively. Quantum state tomography on the generated state shows that the fidelity towards the $|\Phi^+\rangle$ state is 0.991 ± 0.013 [see Fig. 2(c)].

Brightness and pair-to-singles ratios are reduced compared to the larger interferometer-based design which is attributed to scattering losses at the interface of the two parts of the SHWP. This is difficult to overcome since the interface overlaps with the maximum intensity of the pump beam. This also prevents the use of a strongly focused pump to achieve high brightness ($\sim$1 Mc s^{-1}/mW) comparable to the state-of-the-art entangled photon sources [16,19,29]. Improved tolerances in the fabrication of the SHWP should enable a more focused pump, which could improve the coupling of the SPDC emission into the selected collection mode, thus improving the brightness of the source.

IV. CONCLUSION

This source is a good candidate for constructing rugged and compact entangled photon-pair source. Most other sources of entangled photon pairs require interferometers or additional compensation crystals, which usually leads to a larger footprint. An exception is sources based on type-2 SPDC in which the photon pair is split by its momentum components. While such sources are of similar simplicity compared to the source presented in the present work, they exhibit much lower brightness. The same method can be applied for generating entanglement in telecommunication wavelengths as well. Position correlation is independent of spectral and spatial coherence [30], permitting the use of a broadband pump [19], which is left for future investigation. The necessary and sufficient requirement for our method to generate polarization entanglement is photon pairs with initial position correlation. This condition can be found in various processes, such as SPDC in bulk crystals or four-wave mixing in atomic vapors [24,25,31–33]. Applying this effect in atomic vapors could provide another route to observing polarization entangled photons with linewidths compatible with atomic systems. In conclusion, we have demonstrated that the inherent position correlation of the photon pairs generated via SPDC in bulk media is another route for the implementation of compact, high-performing polarization entangled photon-pair sources.

ACKNOWLEDGMENTS

This research was supported by National Research Foundation Award No. R-710-00-133-281 and the Singapore Ministry of Education Research Centres of Excellence program.

[1] D. Bouwmeester, J.-W. Pan, K. Mattle, M. Eibl, H. Weinfurter, and A. Zeilinger, Nature (London) **390**, 575 (1997).

[2] K. Mattle, H. Weinfurter, P. G. Kwiat, and A. Zeilinger, Phys. Rev. Lett. **76**, 4656 (1996).

[3] T. Jennewein, C. Simon, G. Weihs, H. Weinfurter, and A. Zeilinger, Phys. Rev. Lett. **84**, 4729 (2000).

[4] J.-W. Pan, D. Bouwmeester, H. Weinfurter, and A. Zeilinger, Phys. Rev. Lett. **80**, 3891 (1998).

[5] X.-s. Ma, S. Zotter, J. Kofler, R. Ursin, T. Jennewein, C. Brukner, and A. Zeilinger, Nat. Phys. **8**, 479 (2012).

[6] R. Ursin, F. Tiefenbacher, T. Schmitt-Manderbach, H. Weier, T. Scheidl, M. Lindenthal, B. Blauensteiner, T. Jennewein, J. Perdigues, P. Trojek, B. Ömer, M. Fürst, M. Meyenburg, J. Rarity, Z. Sodnik, C. Barbieri, H. Weinfurter, and A. Zeilinger, Nat. Phys. **3**, 481 (2007).

[7] X.-S. Ma, T. Herbst, T. Scheidl, D. Wang, S. Kropatschek, W. Naylor, B. Wittmann, A. Mech, J. Kofler, E. Anisimova, V. Makarov, T. Jennewein, R. Ursin, and A. Zeilinger, Nature (London) **489**, 269 (2012).

[8] J. Yin, Y. Cao, Y.-H. Li, J.-G. Ren, S.-K. Liao, L. Zhang, W.-Q. Cai, W.-Y. Liu, B. Li, H. Dai *et al.*, Phys. Rev. Lett. **119**, 200501 (2017).

[9] P. G. Kwiat, K. Mattle, H. Weinfurter, A. Zeilinger, A. V. Sergienko, and Y. Shih, Phys. Rev. Lett. **75**, 4337 (1995).

[10] P. G. Kwiat, E. Waks, A. G. White, I. Appelbaum, and P. H. Eberhard, Phys. Rev. A **60**, R773 (1999).

[11] P. Trojek and H. Weinfurter, Appl. Phys. Lett. **92**, 211103 (2008).

[12] F. Steinlechner, P. Trojek, M. Jofre, H. Weier, D. Perez, T. Jennewein, R. Ursin, J. Rarity, M. W. Mitchell, J. P. Torres, H. Weinfurter, and V. Pruneri, Opt. Express **20**, 9640 (2012).

[13] A. Villar, A. Lohrmann, and A. Ling, Opt. Express **26**, 12396 (2018).

[14] T. Kim, M. Fiorentino, and F. N. C. Wong, Phys. Rev. A **73**, 012316 (2006).

[15] A. Fedrizzi, T. Herbst, A. Poppe, T. Jennewein, and A. Zeilinger, Opt. Express **15**, 15377 (2007).

[16] F. Steinlechner, M. Gilaberte, M. Jofre, T. Scheidl, J. P. Torres, V. Pruneri, and R. Ursin, J. Opt. Soc. Am. B **31**, 2068 (2014).

[17] M. Fiorentino and R. G. Beausoleil, Opt. Express **16**, 20149 (2008).

[18] L. K. Shalm, E. Meyer-Scott, B. G. Christensen, P. Bierhorst, M. A. Wayne, M. J. Stevens, T. Gerrits, S. Glancy, D. R. Hamel, M. S. Allman, *et al.*, Phys. Rev. Lett. **115**, 250402 (2015).

[19] A. Lohrmann, C. Perumangatt, A. Villar, and A. Ling, Appl. Phys. Lett. **116**, 021101 (2020).

[20] J. Schneeloch and J. C. Howell, J. Opt. **18**, 053501 (2016).

[21] M. P. Edgar, D. S. Tasca, F. Izdebski, R. E. Warburton, J. Leach, M. Agnew, G. S. Buller, R. W. Boyd, and M. J. Padgett, Nat. Commun. **3**, 984 (2012).

[22] M. D'Angelo, Y.-H. Kim, S. P. Kulik, and Y. Shih, Phys. Rev. Lett. **92**, 233601 (2004).

[23] M. N. O'Sullivan-Hale, I. A. Khan, R. W. Boyd, and J. C. Howell, Phys. Rev. Lett. **94**, 220501 (2005).

[24] B. Srivathsan, G. K. Gulati, B. Chng, G. Maslennikov, D. Matsukevich, and C. Kurtsiefer, Phys. Rev. Lett. **111**, 123602 (2013).

[25] C. Shu, P. Chen, T. K. A. Chow, L. Zhu, Y. Xiao, M. M. T. Loy, and S. Du, Nat. Commun. **7**, 12783 (2016).

[26] C. Wagenknecht, C.-M. Li, A. Reingruber, X.-H. Bao, A. Goebel, Y.-A. Chen, Q. Zhang, K. Chen, and J.-W. Pan, Nat. Photon. **4**, 549 (2010).

[27] Z. Tang, R. Chandrasekara, Y. C. Tan, C. Cheng, K. Durak, and A. Ling, Sci. Rep. **6**, 25603 (2016).

[28] A. Lohrmann, C. Perumgatt, and A. Ling, Opt. Express **27**, 13765 (2019).

[29] F. Steinlechner, S. Ramelow, M. Jofre, M. Gilaberte, T. Jennewein, J. P. Torres, M. W. Mitchell, and V. Pruneri, Opt. Express **21**, 11943 (2013).

[30] W. Zhang, R. Fickler, E. Giese, L. Chen, and R. W. Boyd, Opt. Express **27**, 20745 (2019).

[31] G. K. Gulati, B. Srivathsan, B. Chng, A. Cerè, and C. Kurtsiefer, New J. Phys. **17**, 093034 (2015).

[32] K. S. Choi, H. Deng, J. Laurat, and H. J. Kimble, Nature (London) **452**, 67 (2008).

[33] Y. C. Yu, D. S. Ding, M. X. Dong, S. Shi, W. Zhang, and B. S. Shi, Phys. Rev. A **97**, 043809 (2018).